ЖЭТФ, 2016, том 149, вып. 6, стр. 1285–1290

REVERSE DEPLETION EFFECTS AND THE DETERMINATION OF LIGAND DENSITY ON SOME SPHERICAL BIOPARTICLES

Chunxiang Wang [a,b], *Yanhui Liu* [b*], *Yangtao Fan* [b], *Yijun Liu* [b], *Qiancheng Li* [b], *Houqiang Xu* [b**]

[a] *Heilongjiang Bayi Agricultural University*
163319, Daqing, China

[b] *Guizhou University*
550025, Guiyang, China

Received December 4, 2015

In cell environments crowded with macromolecules, the depletion effects act and assist in the assembly of a wide range of cellular structures, from the cytoskeleton to the chromatin loop, which are well accepted. But a recent quantum dot experiment indicated that the dimensions of the receptor–ligand complex have strong effects on the size-dependent exclusion of proteins in cell environments. In this article, a continuum elastic model is constructed to resolve the competition between the dimension of the receptor–ligand complex and depletion effects in the endocytosis of a spherical virus-like bioparticle. Our results show that the depletion effects do not always assist endocytosis of a spherical virus-like bioparticle; while the dimension of the ligand–receptor complex is larger than the size of a small bioparticle in cell environments, the depletion effects do not work and reverse effects appear. The ligand density covered on the virus can be identified quantitatively.

DOI: 10.7868/S0044451016060183

1. INTRODUCTION

Depletion effects are well known to lead to phase separation in the bulk of colloids consisting of large and small particles dominated by short-range repulsive interactions [1–4]. Recently, a highlight experiment demonstrated the depletion effects directly [5]. The trace of a single polystyrene particle in a vesicle was observed on a focal plane under microscopy. When there are no small spheres in the vesicle, the single polystyrene particle freely diffuses all available space in the vesicle. When the vesicle also contains smaller particles, one can see clearly that the larger particle is attracted to the wall of the vesicle. Depletion effects have been applied to nanoparticle-based nanotechnology, such as nanoparticle separation. More recently, Vaia and his colleagues [6] demonstrated a robust and efficient procedure of shape and size selection of Au nanoparticle through the formation of reversible flocculates by a surfactant micelle induced depletion interaction. Depletion effects are also effective in an assembly of colloidal semiconductor nanorods in solution [7]. By tuning depletion attraction forces between hydrophobic colloidal nanorods of semiconductors, dispersed in organic solvent, the nanorods could be assembled into two-dimensional monolayers of closed-packed hexagonally ordered arrays directly in solution.

In cell environments, depletion effects also play an important role, by assisting in the assembly of a wide range of cellular structures, from the cytoskeleton to chromatin loops and whole chromosomes, even the endocytosis of virus [8]. Recent review [9] outlined the interactions that promote bionanoparticle wrapping at the surface membrane: the promotive interactions include specific interaction binding, nonspecific binding, and optimal particle size and shape. The depletion effects should be considered as nonspecific binding. Especially, the recent experiment in [10], based on quantum dots, has demonstrated that the dimension of the ligand–receptor complex has strong effects on the size-dependent exclusion of proteins whose dimension is comparable with the size of small particles in cell environments. By incorporating most of the interactions that promote virus-like particle wrapping at the surface membrane, we have found that the optimal par-

* E-mail: ionazati@itp.ac.cn
** E-mail: houqiangxu@yahoo.com

ticle size and shape depend on the dimension of the ligand–receptor complex and the depletion effects [11].

All the reviews mentioned above prove that the depletion effects always produce attractive force in different systems ranging from colloids to nanobioparticle, even the real cell process. The question of whether the depletion effects always produce attractive forces emerges and deserves to be revolved, especially, under the condition that the dimension of the ligand–receptor complex can be comparable with the size of some small bioparticles in cell environments. Here, a continuum elastic model [10, 12] recently proposed by us is extended to resolve the relationship between the dimensions of the receptor–ligand complex and the depletion effects in endocytosis of virus-like particles and determine the ligand density on some spherical viruses.

2. THEORETICAL MODEL

The resistive and promotive interactions for the bionanoparticle wrapped at the surface membrane outlined in recent review [9] mainly include specific binding (ligand–receptor binding), nonspecific binding (depletion effects), optimal particle size and shape, stretching elasticity of the cell membrane, and so on. During the endocytosis process, the resistive and promotive interactions for the virus-like particle wrapping incorporated into our continuum model are as follows.

2.1. The promotive interactions

The ligand–receptor interaction and depletion effects correspond to the respective specific and nonspecific interactions, both of which belong to the promotive interactions. The interaction energy E_1 caused by the depletion effects originating from entropy is determined by the depletion volume v and the concentration c of small bioparticles in the cell environment and can be expressed as $E_1 = \int p\,dv$, where $p = ck_BT$ [13], and v depends on the dimension δ of the ligand–receptor complex and the radius r of the small bioparticle in the cell environment.

As shown in Fig. 1, when a virus-like particle is approaching the biomembrane, if the dimension of the ligand–receptor complex is not considered, the virus particle overlaps with the biomembrane totally, and the depletion volume should be

$$v = \frac{2\pi h}{3R}\left[(R+2r)^3 - R^3\right].$$

Once the dimension δ of the ligand–receptor complex is considered, the virus-like particle cannot reach the biomembrane infinitely, and a limit gap appears between the virus-like particle and the biomembrane, with its size being the dimension δ of the ligand–receptor complex. Obviously, compared with the case where the dimension of the ligand–receptor complex is not considered, the depletion volume is partially reduced and can be expressed as

$$v = \frac{2\pi h}{3(R+\delta)}\left[(R+2r-\delta)^3 - R^3\right].$$

The nonspecific interaction energy from the depletion effects can be expressed as

$$E_1 = -\frac{2\pi h}{3(R+\delta)}c\left[(R+2r-\delta)^3 - R^3\right], \qquad (1)$$

with k_BT taken as the unit of E_1 and all the energies in the following sections, unless stipulated otherwise.

The specific ligand–receptor interaction is proportional to the adhesion area at the adhesion zone, the density ρ of the ligand–receptor complex, and the binding energy f of the ligand–receptor complex. The ligand–receptor binding energy is estimated to be about of 10–25 [14]. The specific interaction energy is

$$E_2 = -2\pi f\rho h(R+\delta). \qquad (2)$$

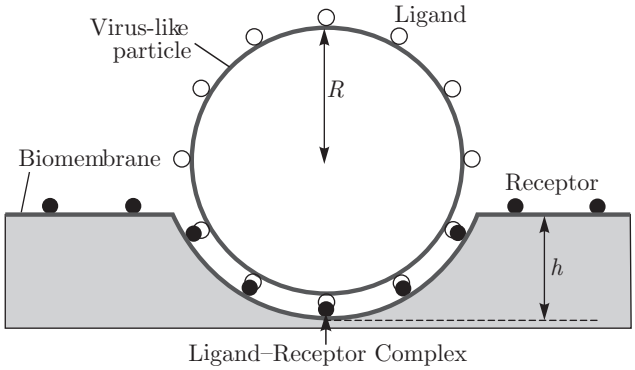

Fig. 1. Representations of the endocytosis process of a virus-like particle and the effects of the dimension of the ligand–receptor complex on the depletion effects. The virus-like particle and the biomembrane including cytoskeleton. The respective white and black circles represent the ligand and receptor. The radius of the virus-like particle, the dimension of the receptor–ligand complex, and the engulfment of the virus-like particle are respectively indicated by R, δ, and h

2.2. The resistive interactions

The resistive energy consists of the elastic recoil of the biomembrane (the bending, stretching energy of the biomembrane) and the elastic energy of the biomembrane, which can be balanced by the thermodynamic

energy generated by the cooperative interactions E_1 and E_2. The elastic recoil of the biomembrane can be described by the Hefrich energy [15]. The energy difference before and after the engulfment can be approximately expressed as

$$E_3 = \frac{4\pi kh}{R+\delta} + \pi\lambda h^2, \tag{3}$$

where k is the bending modulus of the biomembrane, typically of the order of 10–20, and λ is the surface tension of the biomembrane, around $0.005/\text{nm}^2$ [16].

During the process of the virus-like particle being engulfed, the boundary of the adhesion zone can be treated as a circle. Under the condition that the virus-like particle and the biomembrane are uniform and isotropic, the elastic energy of biomembrane can be written as [17]

$$E_4 = \frac{2\pi(R+\delta)^{0.5}h^{2.5}}{5\mu}. \tag{4}$$

Young's modulus and the Poisson ratio of the virus-like particle and the biomembrane can be incorporated into the parameter

$$\mu = \frac{3}{4}\left(\frac{1-\sigma_1^2}{\varepsilon_1} - \frac{1-\sigma_2^2}{\varepsilon_2}\right),$$

in which σ_1 and ε_1 are respectively the Poisson ratio and Young's modulus of the virus-like particle, and σ_2 and ε_2 are those of the biomembrane. Young's modulus of the virus-like particle is much larger than that of the biomembrane, whence

$$\frac{1-\sigma_1^2}{\varepsilon_1} \ll \frac{1-\sigma_2^2}{\varepsilon_2},$$

and therefore μ is only determined by σ_2 and ε_2. Young's modulus of the biomembrane is of the order of 10 kPa or less and the Poisson ratio of the biomembrane is taken to be 0.5, whence

$$\mu = \frac{3}{4}\,\frac{1-\sigma_1^2}{\varepsilon_1} = 256.25.$$

3. RESULTS

3.1. Reverse of depletion effects

Combing all the energies $E_1 \sim E_4$, the total energy can be expressed as

$$E = -2\pi f\rho h(R+\delta) - \frac{2\pi h}{3(R+\delta)}c[(R+2r-\delta)^3 - R^3] + \\ + \frac{4\pi kh}{R+\delta} + \pi\lambda h^2 + \frac{2\pi(R+\delta)^{0.5}h^{2.5}}{5\mu}. \tag{5}$$

The second term in the right-hand side of Eq. (5), indicating the free energy from depletion effects, depends on the concentration and size of small bioparticles in the cell environment and the dimension of the ligand–receptor complex. Especially the expression

$$(R+2r-\delta)^3 - R^3 \tag{5a}$$

indicates the competition between the dimension of the ligand–receptor complex and the size of small bioparticles in the cell environment, determining whether the depletion effects work. When the diameter $2r$ of small bioparticles in the cell environments is larger than the dimension δ of the ligand–receptor complex, the depletion effects produce attractive forces. As shown in Fig. 2*a* (case I), the diameter of a small bioparticle in the cell environment ($2r = 30$ nm) is larger than the dimension of the ligand–receptor complex ($\delta = 20$ nm), which makes the term (5a) to be positive. Hence, the term

$$-\frac{2\pi h}{3(R+\delta)}c\left[(R+2r-\delta)^3 - R^3\right] \tag{5b}$$

is negative, and the total energy E decreases with the concentration of small bioparticles in the cell environment increasing.

Once the diameter of small bioparticles in the cell environment is less than the dimension of the ligand–receptor complex ($2r < \delta$), the small bioparticles can swim freely in the gap between the bioparticle and the biomembrane, and therefore the depletion effects do not work. As shown in Fig. 2*a* (case II), the diameter of a small bioparticle in the cell environment ($2r = 10$ nm) is less than the dimension of the ligand–receptor complex ($\delta = 20$ nm), which makes the term (5a) negative, and hence the term (5b) is positive. Obviously, with the concentration of small bioparticles in the cell environment increasing, the total energy E increases.

The phenomena mentioned in Fig. 2*a* can also be found in Fig. 2*b*, where the diameter of a small bioparticle is $2r = 50$ nm and $2r = 10$ nm, respectively for cases I and II. For both cases, the dimension of the ligand–receptor complex is 40 nm.

3.2. The determination of the ligand density on some spherical bioparticles

The ligand density on a virus-like particle can be determined by the equilibrium state of Eq. (5) and is expressed as

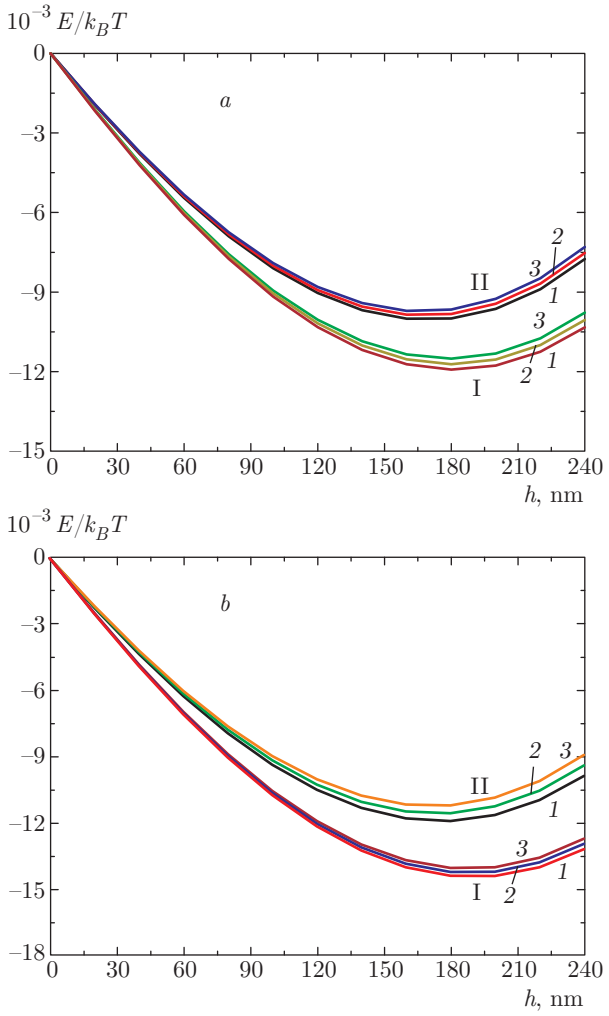

Fig. 2. Dependence of the total energy on depletion effects and reversal of depletion effects. (*a*) In case I, the total energy decreases as the concentration of small bioparticles in the cell environment increases, the diameter of the small bioparticle is $2r = 30$ nm; in case II, the total energy increases as the concentration of small bioparticles in the cell environment increases, $2r = 10$ nm. In both cases, the dimension of the ligand–receptor complex is 20 nm. (*b*) In case I, the total energy decreases as the concentration of small bioparticles in the cell environment increases, $2r = 50$ nm; in case II, the total energy increases as the concentration of small bioparticles in the cell environment increases, $2r = 10$ nm. In both cases, the dimension of the ligand–receptor complex is 40 nm. The curves *1*, *2* and *3* correspond to $c_1 = 0.8 \cdot 10^{-3}$ nm^{-3}, $c_2 = 1.0 \cdot 10^{-3}$ nm^{-3}, and $c_3 = 1.2 \cdot 10^{-3}$ nm^{-3}

$$\rho = \frac{c[(R+2r-\delta)^3 - R^3]}{3f(R+\delta)^2} - \frac{k}{f(R+\delta)^2} - \frac{2\pi\lambda h}{f(R+\delta)} - \frac{h^{1.5}}{2f\mu(R+\delta)^{-0.5}}. \quad (6)$$

The surface ligand density on a virus-like particle is an important factor that provides the specific adhesion in the endocytosis. As shown in Figs. 3*a* and 3*b*, the ligand density strongly depends on the radius of the virus-like particle, the dimension of the ligand–receptor complex, and the ligand–receptor binding energy. Clearly, with the ligand–receptor binding energy increasing, the ligand density decreases.

Figures 3*c* and 3*d* correspond to the ligand density covering the respective Semliki Forest virus and HIV-1 virus. The Semliki Forest virus is a tightly enveloped, roughly spherical, animal virus 70 nm in diameter [18]. The virus is covered by 80 ligands, and therefore its ligand density should be $80/4\pi R^2 = 0.005$ nm^{-2}. For the HIV-1 virus particle, there are 219 gp120 proteins (surface ligand) on its surface [16]. Recent single molecule experiment indicated that the diameter of the HIV-1 virus is about 100 nm [19], whence the density of the surface ligand is $219/4\pi R^2 = 0.007$ nm^{-2}.

According to the quantitative analysis above, two main factors should be addressed. First, as shown in Figs. 3*c* and 3*d*, the ligand density on the Semliki Forest virus and HIV-1 virus is consistent with the theoretical results by the order of magnitude. Second, the quantitative analysis above can help identify the dimension of the ligand–receptor complex; the dimensions of the ligand–receptor complex corresponding to ligand densities 0.005 nm^{-2} and 0.007 nm^{-2} are 28 nm and 40 nm, respectively, both of which fall into the interval between 10 and 45 nm outlined by recent experiment [10].

4. CONCLUSIONS

Generally, depletion effects have been thought to produce an attractive force, but this is not always true. Our results indicate that whether the depletion effects produce attractive forces in the endocytosis of a virus depends on the comparison between the dimension of the ligand–receptor complex and the size of small bioparticles in the cell environment. If the dimension of the ligand–receptor complex is less than the diameter of the bioparticle in the cell environment, the depletion effects work and are advantageous to endocytosis; conversely, the depletion effects become reverse and the endocytosis of a virus does not benefit from depletion effects. These results will highlight the design of the protein corona coated on virus-like particles that transport medicine or others to the target cell. In order to make depletion effects work in the endocytosis of a virus-like particle, the protein corona should be

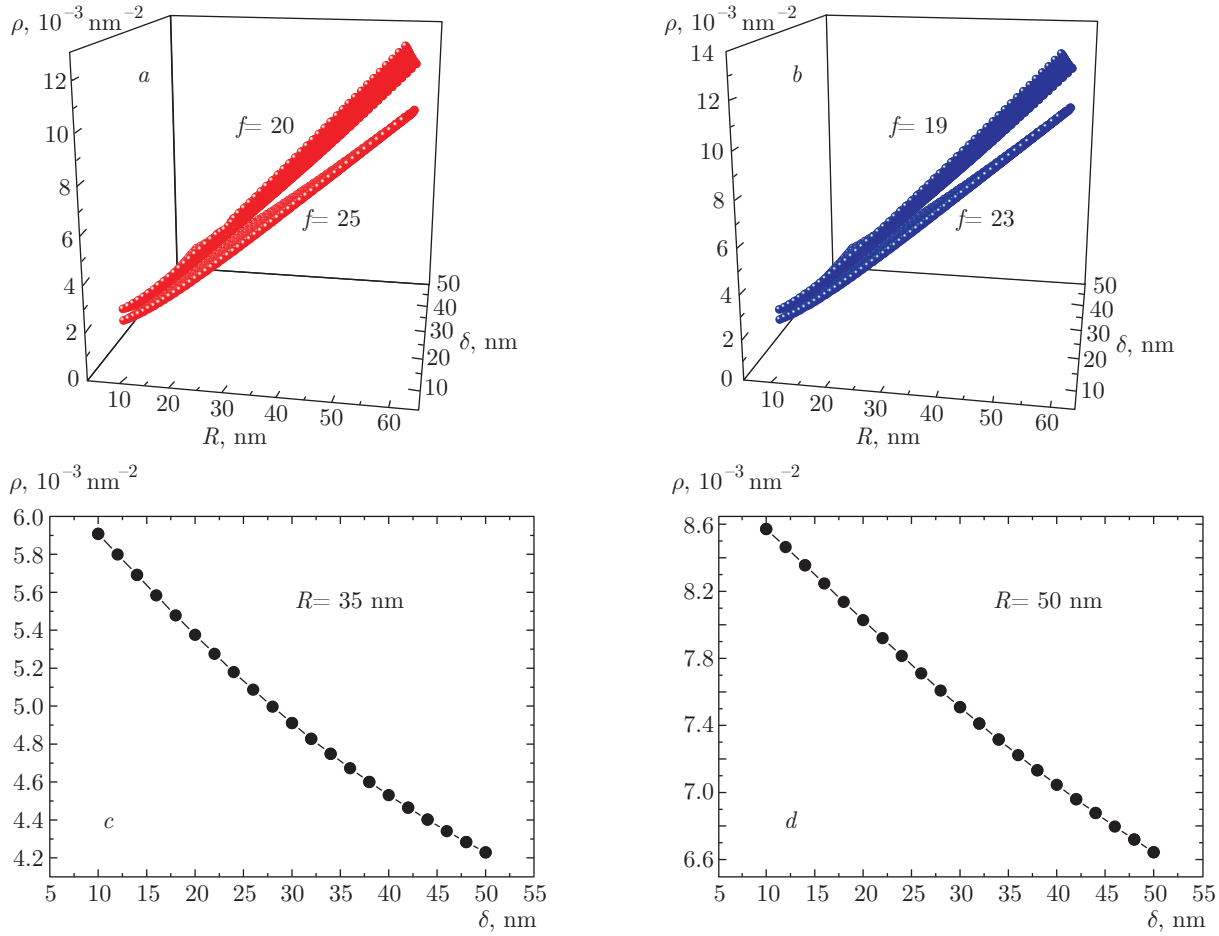

Fig. 3. The dependences of the ligand density in equilibrium on the (a–d) radius of a spherical virus bioparticle and (a,b) dimension of the ligand–receptor complex for the receptor–ligand binding energies (a) 20 and 25 (b) 19 and 23; the ligand density covering (c) the Semliki Forest Virus of the radius 35 nm and (d) the HIV-I Virus of the radius 50 nm

designed less than the diameter of small bioparticles in the cell environment.

As the same time, our results indicate that the ligand density covered on a virus depends on the radius of the virus, the dimension of the ligand–receptor complex, and the ligand–receptor binding energy. From our results, the dimension of the ligand–receptor complex corresponding to the definite ligand density and the radius of the virus can be identified. But the dimension should be proved by experiments further, because the current virus morphology seldom provides the dimension of the ligand–receptor complex.

We acknowledge the support extended by the National Natural Science Foundation of China (11047022, 11204045, 11464004, and 31360215), The Research Foundation from the Ministry of Education of China (2012152), Guizhou provincial tracking key program of social development (SY20123089, SZ20113069), The general financial grant from the China Postdoctoral Science Foundation (2014M562341), the research foundation for young university teachers from Guizhou University (201311), and College innovation talent team of Guizhou province, (2014)32, the West Light Foundation (2015).

REFERENCES

1. J. L. Barrat and J. P. Hansen, *Basic Concepts for Simple and Complex Liquids*, Cambridge Univ. Press, Cambridge (2003).

2. D. Marenduzzo, K. Finan, and P. R. Cook, J. Cell Biol. **175**, 681 (2006).

3. S. Asakura and F. Oosawa, J. Polym. Sci. **33**, 183 (1958).

4. S. Asakura and F. Oosawa, J. Chem. Phys. **22**, 1255 (1954).

5. A. D. Dinsmore, D. T. Wong, P. Nelson, and A. G. Yodh, Phys. Rev. Lett. **80**, 409 (1998).

6. Kyoungweon Park, Hilmar Koerner, and Richard A. Vaia, Nano Lett. **10**, 1433 (2010).

7. D. Baranov, A. Fiore, Marijn van Huis et al., Nano Lett. **10**, 743 (2010).

8. D. Marenduzzo, K. Finan, and P. R. Cook, J. Cell. Biology **175**, 681 (2006).

9. A. E. Nel, L. Madler, D. Velegol et al., Nature Mater. **8**, 543 (2009).

10. Yan-Hui Liu, Yingbing Chen, Wei Mao et al., Front. Phys. **9**, 519 (2014).

11. J.-M. Alakoskela, A. L. Koner, D. Rudnicka et al., Biophys. J. **100**, 2865 (2011).

12. Yingbing Chen, Yan-Hui Liu, Yan Zeng et al., Front. Phys. **10**, 116 (2015).

13. P. Nelson, *Biological Physics, Energy, Information, and Life*, W. H. Freeman and Co., New York–Basingstoke (2007).

14. G. I. Bell, Science **200**, 618 (1978).

15. Z. C. Ouyang, J. X. Liu, and Y. Z. Xie, *Geometric Methods in the Elastic Theory of Membranes in Liquid-Crystal Phase*, World Sci., Singapore (1999).

16. S. X. Sun and D. Wirtz, Biophys. J. **90**, L10 (2006).

17. L. D. Landau and E. M. Lifshitz, *Theory of Elasticity*, Pergamon, Oxford (1986).

18. S. Tzlil, M. Desermo, W. M. Gelbart, and A. Ben-Shal, Biophys. J. **86**, 2037 (2004).

19. N. Kol, Yu Shi, M. Tsvitov et al., Biophys. J. **92**, 1777 (2009).